Electronic Structure of the $[MNH_2]^+$ (M = Sc−Cu) Complexes

Marc F. A. Hendrickx* and Sergiu Clima

Afdeling voor Kwantumchemie en Fysicochemie, Departement Chemie, Katholieke Universiteit Leuven, Celestijnenlaan 200F, B-3001 Heverlee-Leuven, Belgium

Received: April 21, 2006; In Final Form: September 20, 2006

B3LYP geometry optimizations for the $[MNH_2]^+$ complexes of the first-row transition metal cations (Sc^+−Cu^+) were performed. Without any exception the ground states of these unsaturated amide complexes were calculated to possess planar geometries. CASPT2 binding energies that were corrected for zero-point energies and including relativistic effects show a qualitative trend across the series that closely resembles the experimental observations. The electronic structures for the complexes of the early and middle transition metal cations (Sc^+−Co^+) differ from the electronic structures derived for the complexes of the late transition metal cations (Ni^+ and Cu^+). For the former complexes the relative higher position of the 3d orbitals above the singly occupied $2p_\pi$ HOMO of the uncoordinated NH_2 induces an electron transfer from the 3d shell to $2p_\pi$. The stabilization of the 3d orbitals from the left to the right along the first-row transition metal series causes these orbitals to become situated below the HOMO of the NH_2 ligand for Ni^+ and Cu^+, preventing a transfer from occurring in the $[MNH_2]^+$ complexes of these metal cations. Analysis of the low-lying states of the amide complexes revealed a rather unique characteristic of their electronic structures that was found across the entire series. Rather exceptionally for the whole of chemistry, π-type interactions were calculated to be stronger than the corresponding σ-type interactions. The origin of this extraordinary behavior can be ascribed to the low-lying sp^2 lone pair orbital of the NH_2 ligand with respect to the 3d level.

Introduction

Gas-phase experiments have the great advantage of lacking strong intermolecular interactions or crystal forces, so they provide direct insight into the molecular or ionic properties of chemically interesting species. Clemmer et al. have studied gas-phase reactions of first-row transition metal cations with ammonia as a function of translational energy by using a guided ion beam tandem mass spectrometer.[1−4] Among the products of these reactions they obtained $[MNH_2]^+$ species, for which they reported bond energies for the metal ligand bond that, with the exception for Fe^+, are still the experimental reference values. A short time after these experiments were carried out, Harrison et al. performed calculations on these unsaturated amide complexes for the first half (from Sc^+ to Mn^+) of the first-row transition metal series.[5,6] Their study consisted of a detailed investigation of the electronic and geometric structures of $[MNH_2]^+$ by using the generalized valence bond (GVB) method. The calculated binding energies were 7%−38% lower than the experimental values. These deviations from the experimental results should be ascribed to the insufficient treatment of the dynamic electron correlation effects, which are especially important in determining the equilibrium geometries. For the iron complex $[FeNH_2]^+$, only very recently a new experimental binding energy has been reported by Armentrout et al. together with theoretical values obtained by the B3LYP and CCSD(T) computational methods.[4] A good correspondence between theory and experiment was obtained. The ammonia activation reactions of the next member of the first-row transition metal cations, Co^+, was simultaneously and independently investigated on a theoretical basis by Taketsugu et al.[7] and Hendrickx et al.[8] Although in both studies the geometry optimizations were performed at the CASSCF level, different equilibrium structures were obtained. The former study proposed a planar equilibrium structure for the $[CoNH_2]^+$ product, whereas in the latter a nonplanar structure was obtained. In a subsequent publication Taketsugu et al. have calculated at various levels of theory the reactions of Ni^+ and Cu^+ with ammonia; however, no estimations of the binding energies for the $[MNH_2]^+$ amide complexes were reported.[9] More recently, detailed B3LYP theoretical investigations of the activation of ammonia by the singly charged first-row transition metal cations were presented in the literature by Sicilia et al.[10−15] Among other reaction products, they calculated binding energies for the metal ligand bond in the $[MNH_2]^+$ complexes, which are in some cases at variance with the experimental results. In particular, for Cr^+ the difference between B3LYP and experiment is quite large and amounts to as much as 18 kcal/mol. In light of these results and the recent reevaluation of the experimental data for the iron complex,[4] the theoretical results have to be reconsidered at a higher level of theory. Additionally, our wave function approach is able to obtain insight into the true electronic structure of the ground states for these complexes. In this contribution we report estimates of the binding energies for the whole series of first-row transition metal $[MNH_2]^+$ (M = Sc^+−Cu^+) amide complexes by optimizing the geometries with the B3LYP hybrid density functional theory (DFT) method and evaluating the energetics with the CASSCF/CASPT2 wave function technique.

Computational Details

The geometries for the first-row transition metal $[MNH_2]^+$ compounds for several spin multiplicities were optimized at the B3LYP/6-311++G(d,p) level by using the Gaussian program.[16] Starting from nonplanar structures, no symmetry restrictions

* Corresponding author. Fax: +32.16.327992. E-mail: marc.hendrickx@chem.kuleuven.be.

10.1021/jp062452p CCC: $33.50
Published on Web 10/28/2006

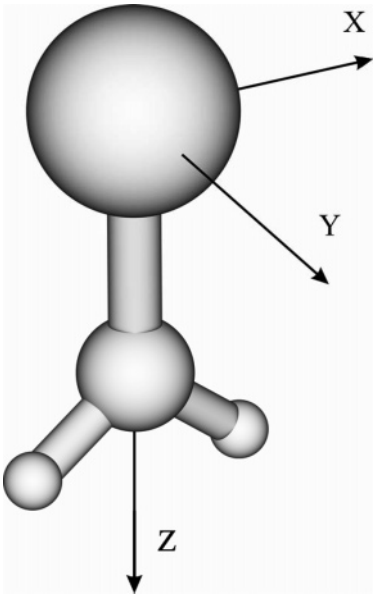

Figure 1. Planar geometry of the $[MNH_2]^+$ complexes with respect to the coordinate system.

were imposed. The nature of all stationary points was identified by performing harmonic vibrational analyses. At the optimized geometries we performed single point ab initio computations by using the CASSCF/CASPT2 method.[17] The newly developed ANO-RCC[18] relativistic basis sets have been used. All the metal cations, the nitrogen atom, and the hydrogen atoms were described by the following number of ANOs: [7s6p4d3f2g], [5s4p3d2f], and [4s3p2d], respectively. At the CASSCF level, we employed an active space that consists of metal 3d, 3d′, and 4s orbitals plus the ligand's upper valence sp^2 lone pair and $2p_\pi$ occupied orbitals, summing to a total of 13 active orbitals. The number of electrons occupying the active space orbitals varied from 5 to 13 in the Sc^+-Cu^+ series. The dynamic correlations were partly recovered at CASPT2 treatment based on the CASSCF wave function by incorporating all valence electrons of N and H and the 3s, 3p, 3d, and 4s electrons of the metal cations. All calculated states are classified according to the irreducible representations of the C_{2v} point group and the coordinate system as drawn in Figure 1. By using the CASPT2 results we can calculate the bonding energy by subtracting from the energy of $[MNH_2]^+$ the sum of the energies of M^+ and NH_2, which were calculated with the full $[MNH_2]^+$ basis set (i.e., counterpoise corrected). To be comparable, the energies of the component parts were calculated at the same level. Relativistic effects were included by using the Douglas−Kroll method, while zero-point-energy corrections (ZPE) to the CASPT2 binding energies were obtained at the B3LYP level of theory.

Results and Discussion

The B3LYP results for the geometry optimization for several low-lying spin multiplicities of the various amide complexes are collected in Table 1. For the lowest spin multiplicity state of each complex, the M−N bond distance decreases along the series from 1.894 Å for $[ScNH_2]^+$ to 1.791 Å for $[CoNH_2]^+$, which possesses the shortest metal ligand bond. For $[NiNH_2]^+$ and $[CuNH_2]^+$ the M−N bond distance increases to 1.829 and 1.861 Å, respectively. Contrary to the metal ligand bond, the internal ligand N−H bond of NH_2 does not change much for the various complexes. The shortest N−H bond (1.016 Å) was found for $[MnNH_2]^+$, while the longest one (1.024 Å) was obtained for $[CuNH_2]^+$. The bond angle in the ligand varies from 107.28° to 110.60°. The smaller angles are found for complexes of the early transition metal cations (Sc^+-Cr^+), whereas the larger angles occur near the end of the series (Mn^+-Cu^+). Also given in Table 1 are the results of the harmonic vibrational analyses. As can been seen, for all studied complexes we calculated real frequencies, indicating that the given structures represent true minima on the potential energy surfaces.

TABLE 1: B3LYP Geometries (Å, deg), Harmonic Vibrational Frequencies (cm^{-1}), and Relative Energies (cm^{-1}) for Several Low-Lying Spin Multiplicities of $[MNH_2]^+$ Complexes of the First-Row Transition Metal Series

		M−N	N−H	∠(H, N, H)	vibrational frequencies						B3LYP+ZPE
$[ScNH_2]^+$	doublet	1.894	1.022	107.28	438	603	692	1532	3457	3542	0
	quartet	2.312	1.028	107.06	351	470	629	1550	3397	3478	16809
$[TiNH_2]^+$	singlet	1.848	1.020	109.63	449	616	727	1505	3468	3556	8512
	triplet	1.855	1.020	108.63	540	627	698	1507	3473	3561	0
	quintet	2.238	1.027	107.16	367	507	638	1555	3402	3479	15394
$[VNH_2]^+$	doublet	1.814	1.020	109.10	555	656	747	1562	3457	3540	8288
	quartet	1.831	1.021	108.90	625	655	671	1552	3457	3542	0
	sextet	2.182	1.027	107.50	366	523	697	1554	3401	3481	11011
$[CrNH_2]^+$	triplet	1.804	1.019	109.63	569	610	720	1556	3470	3560	19715
	quintet	1.852	1.021	108.21	579	586	651	1557	3458	3539	0
	septet	2.177	1.026	107.45	366	534	620	1554	3417	3498	8224
$[MnNH_2]^+$	quartet	1.850	1.024	107.91	520	691	713	1585	3415	3485	12845
	sextet	1.827	1.016	110.47	342	625	700	1522	3507	3600	0
	octet	2.320	1.028	107.21	298	479	697	1541	3388	3478	11518
$[FeNH_2]^+$	triplet	1.854	1.024	108.10	500	643	675	1580	3420	3498	6877
	quintet	1.805	1.018	110.60	473	625	679	1526	3489	3582	0
	septet	2.038	1.028	108.09	337	509	715	1543	3386	3476	14362
$[CoNH_2]^+$	doublet	1.737	1.024	108.68	648	714	747	1561	3424	3508	13651
	quartet	1.791	1.019	110.28	579	650	687	1566	3472	3564	0
	sextet	2.106	1.028	108.75	314	527	723	1528	3380	3475	16509
$[NiNH_2]^+$	singlet	1.724	1.025	108.55	428	660	728	1564	3412	3496	6717
	triplet	1.829	1.022	109.66	573	660	660	1553	3448	3539	0
	quintet	2.071	1.028	109.63	350	553	754	1529	3377	3478	15628
$[CuNH_2]^+$	doublet	1.861	1.024	109.59	492	641	643	1549	3435	3524	0
	quartet	2.026	1.029	111.62	375	557	758	1496	3366	3479	25492

TABLE 2: Relative Energies (cm^{-1}) with Respect to the Ground State and Leading Configurations in the CASSCF Wave Function for Several Low-Lying States of $[MNH_2]^+$ Complexes

	state	ΔE	$8a_1$	$3b_2$	$9a_1$	$10a_1$	$4b_1$	$1a_2$	$4b_2$
$[ScNH_2]^+$	$^2A_1$	0	2	2	1	0	0	0	0
	$^2A_1$	1444	2	2	0	1	0	0	0
	$^2B_1$	2568	2	2	0	0	1	0	0
	$^2B_2$	7578	2	2	0	0	0	0	1
	$^2A_2$	319	2	2	0	0	0	1	0
$[TiNH_2]^+$	$^3A_1$	0	2	2	1	1	0	0	0
	$^3B_1$	278	2	2	1	0	1	0	0
	$^3B_2$	41	2	2	0	0	1	1	0
	$^3A_2$	239	2	2	0	1	0	1	0
$[VNH_2]^+$	$^4A_1$	5815	2	2	0	0	1	1	1
	$^4B_1$	0	2	2	1	1	1	0	0
	$^4B_2$	517	2	2	1	0	1	1	0
	$^4A_2$	1524	2	2	1	1	0	1	0
$[CrNH_2]^+$	$^5A_1$	5757	2	2	1	0	1	1	1
	$^5B_1$	10383	2	2	1	1	0	1	1
	$^5B_2$	0	2	2	1	1	1	1	0
	$^5A_2$	12058	2	2	1	1	1	0	1
$[MnNH_2]^+$	$^6A_1$	0	2	2	1	1	1	1	1
	$^6B_1$	28517	2	1	1	1	1	2	1
	$^6B_2$[a]	11838	2	2	1	1	1	1	0
	$^6A_2$	27448	2	1	1	1	2	1	1
$[FeNH_2]^+$	$^5A_1$	0	2	2	2	1	1	1	1
	$^5B_1$	1261	2	2	1	1	2	1	1
	$^5B_2$	6727	2	2	1	1	1	1	2
	$^5A_2$	165	2	2	1	1	1	2	1
$[CoNH_2]^+$	$^4A_1$	2956	2	2	2	2	1	1	1
	$^4B_1$	0	2	2	2	1	2	1	1
	$^4B_2$	20	2	2	1	1	2	2	1
	$^4A_2$	2819	2	2	1	2	1	2	1
$[NiNH_2]^+$	$^3A_1$	6287	2	1	2	2	2	2	1
	$^3B_1$	1427	2	2	2	2	2	1	1
	$^3B_2$	0	2	2	2	1	2	2	1
	$^3A_2$	406	2	2	2	2	1	2	1
$[CuNH_2]^+$	$^2A_1$	16177	2	2	2	1	2	2	2
	$^2B_1$	24539	2	2	2	2	1	2	2
	$^2B_2$	0	2	2	2	2	2	2	1
	$^2A_2$	25271	2	2	2	2	2	1	2

[a] An additional unpaired electron occupies the $11a_1$ (4s) orbital.

These frequencies should prove to be useful for future characterization in the gas phase of the unsaturated complexes at hand. On the basis of these harmonic vibrational analyses, the B3LYP total energies were corrected for the zero-point energies. The obtained energy differences between the various possible spin multiplicity states of a specific complex are shown in the last column of Table 1. The smallest difference is found in the case of the $[NiNH_2]^+$ complex, but is still larger than 19 kcal/mol. This justifies the limitation of our CASPT2 calculations to the lowest energy spin multiplicity for obtaining the binding energies of the various $[MNH_2]^+$ complexes. For a given state spin multiplicity the CASPT2 energies are calculated for the four irreducible representations of the C_{2v} point group of the planar B3LYP equilibrium structures. Their relative energies expressed in wavenumbers are collected in Table 2. The composition of the leading configuration in the CASSCF wave function expansion is given on the right-hand side of this table. Graphical representations of the corresponding active space orbitals are depicted in Figure 2.

$[ScNH_2]^+$ has previously been discussed in several theoretical investigations on the electronic and geometric structures of all possible products of the reaction of Sc^+ with NH_3.[5,9,14] It is well-known that the $4s^13d^1$ electronic configuration of Sc^+ gives rise to a ^3D ground state. As can be seen from Table 2, our CASPT2//B3LYP calculations predict that it forms with the $(sp^2)^2(2p_\pi)^1$ ($^2B_2$) ground state of NH_2 a planar C_{2v} $^2A_1$ ground state for the $[ScNH_2]^+$ cation. Figure 2 clearly shows that the $2p_\pi$ ($3b_2$) orbital on nitrogen becomes doubly occupied in the complex. The ground-state wave function is made up for about 90% of a single Slater determinant with one unpaired electron in the $9a_1$ molecular orbital that is mainly a $3d_{x^2-y^2}$ metal orbital. At some 4 kcal/mol above this state a second $^2A_1$ is situated, in which the unpaired electron of the doublet state occupies a molecular orbital ($10a_1$) that is a strong admixture of $3d_{z^2}$ and 4s. The two orbitals of the complex are depicted in Figure 2. The common factor of all low-lying states of $[ScNH_2]^+$ in Table 2 is that they correspond formally to a transfer of one electron from Sc^+ to the NH_2 ligand, leaving one electron in a valence metal orbital. A Mulliken population analysis for the ground state shows a net charge on scandium of only +1.18, which is a clear indication that accompanying this formal transfer there is a σ and π donation from the amide ligand to the metal 3d orbitals. Figure 2 shows that this mainly occurs in the $8a_1$ and

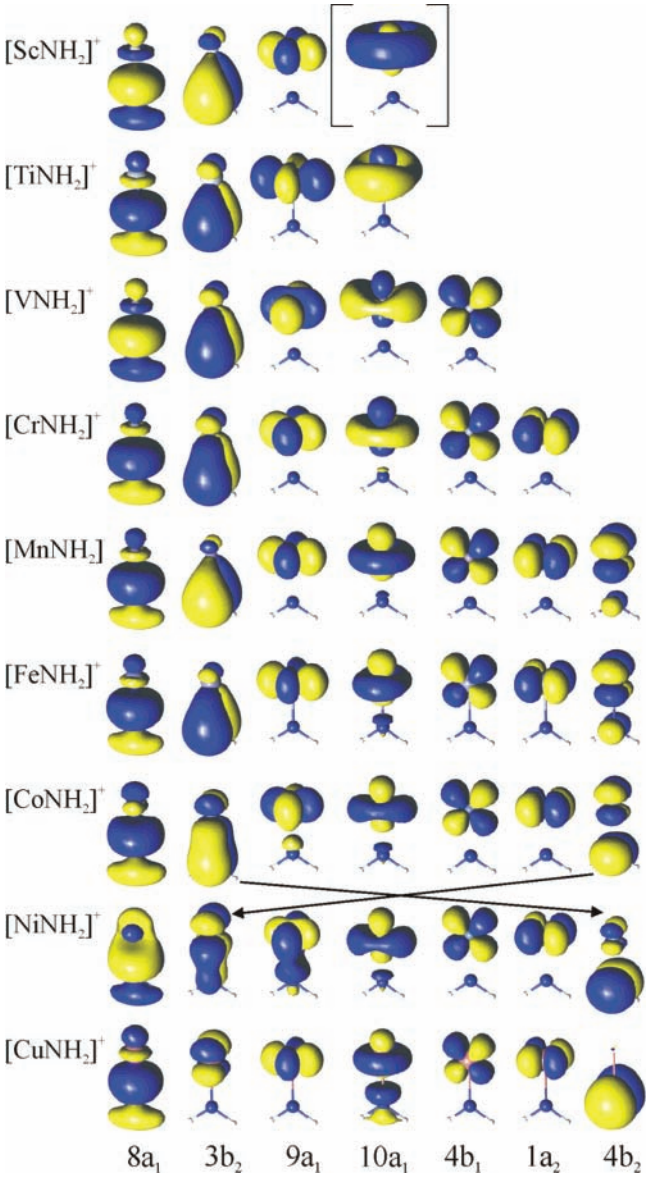

Figure 2. Active space orbitals (as listed in Table 2) that are occupied in the leading configuration of the ground states. The $10a_1$ orbital of $[ScNH_2]^+$ is placed in brackets because it is only occupied in the excited $^2A_1$ state.

TABLE 3: CASPT2 and Experimental Binding Energies (kcal/mol) for the First-Row Transition Metal $[MNH_2]^+$ Complexes

	state	CASPT2	expt[a]
$[ScNH_2]^+$	$^2A_1$	82.45	82.9 ± 2.3
$[TiNH_2]^+$	$^3A_1$	83.40	82.8 ± 3.0
$[VNH_2]^+$	$^4B_1$	79.13	70.0 ± 1.4
$[CrNH_2]^+$	$^5B_2$	61.01	65.1 ± 2.3
$[MnNH_2]^+$	$^6A_1$	57.58	61 ± 5
$[FeNH_2]^+$	$^5A_1$	70.32	66.4 ± 2.8[b]
$[CoNH_2]^+$	$^4B_1$	73.01	58.9 ± 3.2
$[NiNH_2]^+$	$^3B_2$	61.22	53.2 ± 1.8
$[CuNH_2]^+$	$^2B_2$	51.64	45.9 ± 3

[a] At 0 K, ref 19. [b] Reference 4.

$3b_2$ orbitals, since both these predominantly ligand orbitals exhibit strong contributions of $3d_{z^2}$ and $3d_{yz}$, respectively. We therefore conclude that there is to some extent a double bond between the metal cation and the ligand in this complex, which explains its planar geometry. The bonding energy of the ground state has been calculated at the generalized valence bond (GVB) level as 79 kcal/mol,[5] while more recently a value of 80.3 kcal/mol was obtained with the B3LYP method.[10] We calculated a binding energy of 82.45 kcal/mol (ZPE and basis set superposition corrected). Table 3 shows that this value compares quite well with the experimentally proposed bond energy of 82.9 ± 2.3 kcal/mol.[19]

The $[TiNH_2]^+$ $^3A_1$ ground state wave function shows a singly occupied orbital of metal $d_{x^2-y^2}$ nature and a second one that quite well resembles the open shell orbital of the excited $^2A_1$ state of the Sc^+ complex, i.e., an admixture of metal 4s and $3d_{z^2}$. From an analysis of the expansion coefficients of the corresponding molecular orbitals, we concluded that the contribution of 4s has decreased from 65% in $[ScNH_2]^+$ to 50% in the Ti^+ complex. This is in line with the well-known fact that the 3d orbitals are stabilized with respect to the 4s orbital when going from left to right in the first-row transition metal series. As in the case of the Sc^+ complex, the open shell nature of the ground state is located almost entirely on the metal cation, implying again a formal transfer of one electron from Ti^+ to the NH_2 ligand. The experimental value for the binding energy equals nearly the one for the Sc^+ complex, but with a larger error margin: 82.8 ($\pm$3.0) kcal/mol.[2] Our CASPT2 calculations predict a value of 83.4 kcal/mol, which is well within the experimental error margin. The previously calculated B3LYP value of 74.6 kcal/mol[10,13] is significantly lower, although the two computational techniques found the same ground state. Indeed, a Mulliken population analysis arrived in both cases at a total occupation of the 3d orbitals of almost 2.5 electrons. This value implies a combined σ and π donation of half an electron, which mainly takes place in the $8a_1$ and $3b_2$ orbitals. Figure 2 shows that both these orbitals have a predominant ligand character, sp^2 lone pair and $2p_\pi$, respectively, and are of the bonding type with respect to the metal ligand bond. This means that the 3d shell of the metal is situated at a higher energy than the ligand orbitals, which is generally the case in transition metal chemistry. The binding energy of 69.2 kcal/mol as calculated by Harrison et al. deviates even further from our result and the experimental value.[6] This substantial underestimation of the binding energy by the GVB method is the outcome of an insufficient incorporation of dynamic electron correlation, which yields an energy for the complex that is too high in comparison with the sum of the GVB energies of the two separated Ti^+ and NH_2 moieties. Also, their $^3B_1$ GVB ground state is at variance with our CASPT2 results and the B3LYP study of Sicilia et al.[10,13] This finding is nevertheless acceptable as the energy differences between the various low-lying states are extremely small. Indeed, Table 2 shows that three excited triplets states are situated not more than 1 kcal/mol above the ground state, which makes the prediction of the true ground state of the $[TiNH_2]^+$ complex a very demanding task. Further on, from the composition of the wave functions of these states in Table 2, we can conclude that the following 3d orbitals are nearly degenerate: $9a_1$ ($3d_{x^2-y^2}$), $1a_2$ ($3d_{xy}$), and $4b_1$ ($3d_{xz}$). The first two atomic metal orbitals are mainly $3d_\delta$ orbitals, while the last one is a $3d_\pi$ orbital. Since the latter has no counterpart on the NH_2 ligand, all three orbitals are spectator orbitals with respect to the metal ligand bond forming process. They are to a high degree nonbonding orbitals.

According to Table 2 the ground state of $[VNH_2]^+$ is calculated by the CASPT2 method as $^4B_1$, which again formally corresponds with the transfer of an electron from V^+ to the singly occupied $2p_\pi$ orbital of NH_2 and subsequent compulsory spin coupling. Although this bond forming process is also found in the two previous theoretical studies of this unsaturated complex,[6,13] the precise electronic structures of the predicted ground states are more or less different. The GVB study predicted the $^4B_2$ as the lowest state for this complex.[6] In light of our present results this is explicable, since the difference between the two states is about 1.5 kcal/mol at the CASPT2 level (Table 2). More extensive calculations might invert the relative positions of the two states again. The electronic configuration of the $^4B_2$ state as derived from the CASSCF wave function and the GVB calculation of ref 6 corresponds to $(3d_{x^2-y^2})^1$ $(3d_{xz})^1$ $(3d_{xy})^1$, while the electronic configuration of the $^4B_1$ ground state is as follows: $(3d_{x^2-y^2})^1$ $(3d_{xz})^1$ $(3d_{z^2})^1$. Because the energy difference between both states is quite small, we must rather surprisingly conclude that the d_{z^2} orbital as a σ antibonding orbital is nearly degenerate with the $3d_\delta$ ($3d_{x^2-y^2}$, $3d_{xy}$) and $3d_{xz}$ nonbonding orbitals. This conclusion, which is also demonstrated by the small excitation energy to the $^4A_2$ state of the $(3d_{x^2-y^2})^1$ $(3d_{xy})^1$ $(3d_{z^2})^1$ configuration, will be explained later. The relatively high excitation energy of the $^4A_1$ state of the configuration $(3d_{xz})^1$ $(3d_{yz})^1$ $(3d_{xy})^1$, on the other hand, implies a rather high-lying $3d_{yz}$ orbital as a consequence that it is the antibonding counterpart of the bonding $3b_2$ ligand ($2p_\pi$) orbital. This observation also accounts for the high excitation energy of the $^2B_2$ ($(3d_{yz})^1$) state of $[ScNH_2]^+$ in Table 2. All these theoretical findings are gathered in a qualitative orbital diagram as depicted in Figure 3a. At the CASPT2 level we find a binding energy of 79.13 kcal/mol for the V^+-NH_2 bond. This is considerably higher than the measured value of 70.0 ($\pm$1.4) kcal/mol and the previous theoretical values obtained with GVB (66 kcal/mol)[6] and B3LYP (69.0 kcal/mol).[10] The low value in the case of B3LYP is understandable since this study proposed the $^4A_1$ as the ground state, precisely our rather high-lying excited $(3d_{xz})^1$ $(3d_{yz})^1$ $(3d_{xy})^1$ state. The insufficient treatment of electron correlation by the GVB method is again responsible for the low value of the binding energy as obtained by this method.

As for the early first-row transition metal cations, the $2p_\pi$ orbital is again doubly occupied in the ground state of $[CrNH_2]^+$, which means that there remain four valence electrons to be distributed among the five 3d orbitals. On the basis of the relative orbital energies that we derived for these metal orbitals in the previous paragraph, we can anticipate a $^5B_2$ ground state arising from a $(3d_{z^2})^1$ $(3d_{x^2-y^2})^1$ $(3d_{xz})^1$ $(3d_{xy})^1$ electron configuration. Indeed, in this state the strongly antibonding orbital $3d_{yz}$ of Figure 3a is not occupied. Table 2 confirms this ground state for the $[CrNH_2]^+$ complex. The only way to obtain another

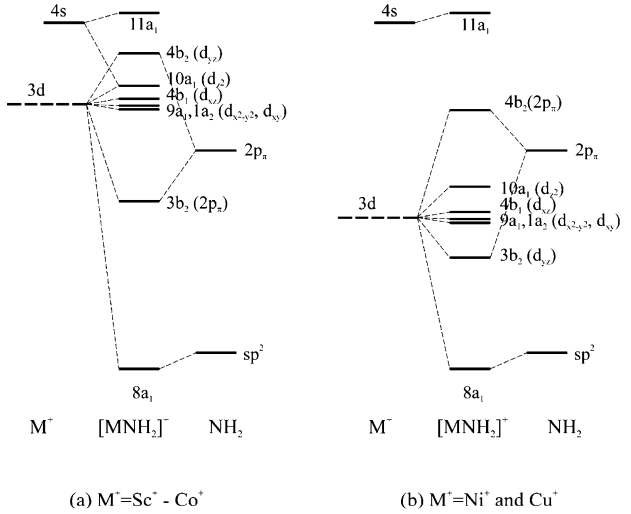

(a) M^+=Sc^+ - Co^+ (b) M^+=Ni^+ and Cu^+

Figure 3. Qualitative orbital diagrams for the $[MNH_2]^+$ complexes of early and middle transition metal cations (a) and of late transition metal cations (b).

quintet state of $3d^4$ configuration involves the occupation of $3d_{yz}$, and therefore all resulting excited states are positioned at energies higher than 5000 cm^{-1}. Table 3 shows a CASPT2 binding energy for this complex of 61.01 kcal/mol, a result that corresponds rather well with the experimental value of 65.1 (±2.3) kcal/mol. Although the same ground state was found at the GVB level of theory in ref 6, the calculated binding energy of 40 kcal/mol is, as for the other amide complexes of Ti^+ and V^+, too small. On the other hand, the B3LYP study[10,13] proposed a different ground state: $^5A_1$. Although it is the second lowest CASPT2 state for this complex in Table 2, the rather large associated excitation energy of more than 16 kcal/mol at the CASPT2 level casts some serious doubt on the result of ref 10. Since apparently a relatively high-lying excited state was incorrectly taken for the ground state of the complex, it is logical that the corresponding binding energy of 48.8 kcal/mol[10] is by far too small (more than 16 kcal/mol) when compared to the experimental and CASPT2 values.

The transfer of an electron from the Mn^+ cation to the NH_2 ligand leaves five metal valence electrons to be distributed over the five 3d orbitals on the metal. The only sextet state possible has therefore each 3d orbital occupied by one electron giving rise to a $^6A_1$ state, precisely the CASPT2 ground state in Table 2. The other sextet states mentioned in Table 2 either demand only one electron in the low-lying $2p_\pi$ orbital of NH_2 and therefore six electrons in the higher lying metal 3d orbitals ($^6B_1$ and $^6A_2$), or demand two electrons in $2p_\pi$ of NH_2, one electron in 4s ($11a_1$) of the metal, and no electrons in the strongly antibonding $3d_{yz}$ ($^6B_2$). Both electronic configurations are clearly energetically unfavorable as witnessed by the rather high excitation energies for these excited states in Table 2. The binding energy for $[MnNH_2]^+$ is measured with an exceptionally high uncertainty of 5 kcal/mol as 61 kcal/mol. Our computed binding energy of 57.58 kcal/mol falls within the experimental uncertainty interval and therefore confirms the experimental value. The GVB[6] and B3LYP[10] studies arrived at binding energies that are substantially smaller, i.e., 43 and 52.6 kcal/mol, respectively. The GVB result is understandable on the basis of its ineffective treatment of electron correlation and should logically be rejected. The nature of the B3LYP ground state is, in our judgment of the available information, acceptable. So far the CASPT2 binding energies and the experimental proposed values show a decreasing trend when going from Sc^+ to Mn^+. The same trend is followed by the previous GVB[6] and B3LYP[10] studies, as can be deduced from Figure 4.

All low-lying quintet states of $[FeNH2]^+$ in Table 2 have a formal $3d^6\ 2p_{\pi^2}$ occupation, which implies a double occupation of just one 3d orbital. The two lowest states, i.e., $^5A_1$ and $^5A_2$, are nearly degenerate with an energy difference between them of less than 0.5 kcal/mol. The reason for this is the double occupation of a single $3d_\delta$ orbital, $3d_{x^2-y^2}$ in the case of the $^5A_1$

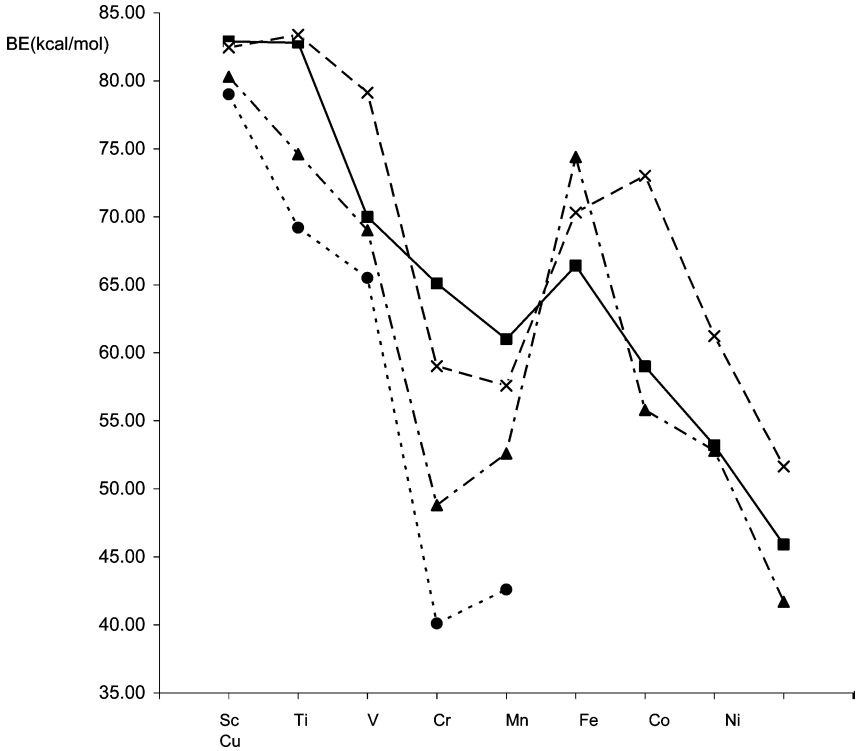

Figure 4. Binding energies of first-row transition metal $[MNH_2]^+$ complexes: experimental results (—■—), present work CASPT2 (— —×— —), Sicilia et al. B3LYP[10] (· — ▲ThinSpace— ·), and Mavridis et al. GVB[6] (--●--).

ground state and $3d_{xy}$ in the $^5A_2$ state. The $^5B_2$ is the highest of the low-lying states because it involves a double occupation of the strong antibonding $4b_2$ ($3d_{yz}$) orbital. These results of our CASPT2 calculations agree nearly completely with a very recent CCSD(T)/6-311++G(3df,3p)//B3LYP/6-311+G* study by Armentrout et al.[4] The geometry of their $^5A_1$ state is to a very high degree identical to our geometry as tabulated in Table 1. Indeed, the only difference between their B3LYP geometry optimizations and ours is the slightly larger basis set used by us. The same two nearly degenerate states ($^5A_1$ and $^5A_2$) and corresponding electronic configurations as described in Table 2 were found. Also, the qualitative classification of the various metal orbitals as either essentially nonbonding ($3d_{x^2-y^2}$, $3d_{xy}$, $3d_{xz}$, $3d_{z^2}$) or strong antibonding ($3d_{yz}$) is given. Thus $3d_{z^2}$, which has symmetry-wise the capability of having a strong σ antibonding interaction with the sp^2 lone pair on NH_2, is rather surprisingly categorized as an essential nonbonding orbital. However, this is in full agreement with our findings for the amide complexes of the early transition metal M^+ cations that were discussed extensively in previous paragraphs. In analyzing the results of ref 4, one should bear in mind that a different position of the molecule with respect to the coordinate system was chosen by the authors. The $^5A_2$ state that is nearly degenerate with the our ground state was found to distort just slightly to a bent structure with a dihedral H−Fe−N−H angle of 176.8° and with a CCSD(T) energy only a few hundredths of a kilocalorie per mole lower than that of the $^5A_1$ state. Therefore, the authors rightfully conclude that higher levels of theory might lead to a planar geometry for the ground state of $[FeNH_2]^+$. Their binding energy of 67.8 kcal/mol at the CCSD(T) level after correcting for ZPE and spin−orbital coupling effects (1.20 kcal/mol) corresponds well with our CASPT2 value of 70.32 kcal/mol. On the basis of their theoretical results, Armentrout et al. reexamined their experimental data and lowered the experimental binding energy from 73.9 (±2.3) kcal/mol[19] to 66.4 (±2.8) kcal/mol.[4] In agreement with our CASPT2 calculations, the B3LYP value of 74.4 kcal/mol as proposed by Sicilia et al.[10] is noticeably higher than the new experimental value (Figure 4).

The B3LYP geometry optimization for $[CoNH_2]^+$ yielded a planar structure opposed to the bent ground-state structure we obtained previously with the CASSCF technique,[8] but in accordance with a recent B3LYP study.[10] Another CASSCF study performed with a different active space and basis set found a planar lowest equilibrium structure, with a $^6A_1$ ground state at the CASSCF level and a $^2A_1$ ground state at the MR-SDCI level.[7] The present B3LYP calculations and the previous B3LYP study[10] agree on a quartet ground state. Further agreement between the two sets of B3LYP calculations is found in a Co−N distance that is slightly smaller than 1.80Å, as opposed to our previous CASSCF bond length of 1.86 Å[7] and the rather large bond distance of 2.17 Å of the sextet CASSCF ground state of ref 8. Table 2 shows a $^4B_1$ ground state with a $^4B_2$ state a merely 20 cm^{-1} higher. This small difference in energy is the outcome of the different occupations of the $3d_\delta$ orbitals, which are essentially nonbonding orbitals and therefore nearly degenerate. The $^4A_1$ and $^4A_2$ states are situated much higher in energy, apparently as the consequence of the occupation of the $10a_1$ (d_{z^2}) orbital (Table 2). This is at variance with the amide complexes of the early transition metal cations, where this orbital was considered nonbonding. In the $[CoNH_2]^+$ complex this has changed and the fairly large excitation energies for $^4A_1$ and $^4A_2$ imply to some degree a more pronounced antibonding interaction between d_{z^2} and the sp^2 lone pair orbital on NH_2. In agreement with the other complexes discussed so far, the $4b_2$ orbital, which is mainly $2p_\pi$ on NH_2, remains doubly occupied. By comparing this orbital in the different complexes in Figure 2, we can clearly see an increase in covalency when going from $[MnNH_2]^+$ to $[CoNH_2]^+$. The reason for this increase in σ ($10a_1$) and π ($4b_2$) covalency is the stabilization of the 3d orbitals along the first-row transition metals which energetically positions them for Co^+ closer to the valence ligand orbitals of NH_2 and to the $2p_\pi$ orbital of this ligand in particular. The antibonding nature of the 3d orbitals signifies that they are situated higher in energy than $2p_\pi$ and consequently much higher than the sp^2 lone pair orbital. Indeed, the $2A_1$ ($(2sp^2)^1$ $(2p_\pi)^2$) excited state of the uncoordinated NH_2 is experimentally known to be 32 kcal/mol higher than the $^2B_2$ ($(sp^2)^2$ $(2p_\pi)^1$) ground state.[20] This fact explains why the σ interactions in the amide complexes discussed so far are weaker than the π interactions. As shown in Figure 4, our calculated binding energy of 73.01 kcal/mol deviates substantially by more than 14 kcal/mol from the experimentally proposed value of 58.9 (±3.2) kcal/mol. The B3LYP calculations of Sicilia et al. gave a $^4A_1$ ground state with a binding energy that is even smaller: 55.8 kcal/mol. This is understandable in light of the fact that we predict this state to be an excited state approximately 8.5 kcal/mol above the $^4B_1$ ground state. In view of the large discrepancy between experiment and theory, further study into the matter from both sides is clearly necessary.

The ground state of the $[NiNH_2]^+$ complex is a $^3B_2$ that has an electronic configuration of $(d_{x^2-y^2})^2$ $(3d_{z^2})^1$ $(3d_{xz})^2$ $(3d_{yz})^2$ $(3d_{xy})^2$ $(2p_\pi)^1$. The most striking difference from the amide complexes discussed so far is the single occupation of $4b_1$ ($2p_\pi$ of NH_2). In fact, together with the $10a_1$ (d_{z^2}) metal orbital these are the only singly occupied orbitals in the ground state, indicating that they are antibonding in nature. Figure 2 illustrates that this is particularly true for the $4b_2$ ($2p_\pi$) orbital, while the corresponding orbital $3b_2$ ($3d_{yz}$) of π symmetry has become a strongly covalent bonding orbital. The σ-type interactions remain, however, the same as for the complexes of the early and middle transition metal complexes ($Sc^{+-}Co^+$), i.e., bonding for the sp^2 lone pair orbital of NH_2 ($8a_1$ in Figure 2) and antibonding for the d_{z^2} orbital ($10a_1$). These observations demonstrate that the 3d shell of Ni^+ is now situated below the $2p_\pi$ orbital of NH_2, but still above the sp^2 lone pair orbital on N as depicted in Figure 3b. The energetically highest positioned orbitals are $4b_2$ and $10a_1$, which are indeed singly occupied in the ground state. All low-lying excited states of $[NiNH_2]^+$ in Table 2 have a single electron in the $2p_\pi$ orbital. The highest lying of these states, the $^3A_1$, has as expected a second unpaired electron in the lowest of the 3d orbitals of Figure 3b, namely $3d_{yz}$ ($3b_2$). The lower lying states $^3A_2$ and $^3B_1$ have a second unpaired electron in one of the nonbonding orbitals, i.e., $3d_{xz}$ ($4b_1$) and $3d_{xy}$ ($1a_2$), respectively. The B3LYP study found a binding energy for the $[NiNH_2]^+$ complex of 52.8 kcal/mol for an extremely slightly bent $^3A'$ ground state, which corresponds to either our $^3A_1$ or $^3B_1$ excited state.[10] Table 2 shows that the CASPT2 binding energy of 61.22 kcal/mol is 8 kcal/mol larger than the experimentally proposed value of 53.2 (±1.8 kcal/mol). Further improvement of the computational level by incorporating more dynamic electron correlation will most likely bring the binding energy more in line with experiment, although a somewhat larger experimental value should also be taken into consideration. Further work is clearly needed.

For $[CuNH_2]^+$ we have to distribute 13 electrons among the seven valence orbitals. We can exclude the 4s orbital from our consideration since for Cu^+ it is positioned at much higher

energies with respect to the 3d level. This implies a doublet ground state with the unpaired electron in the highest orbital, which according to Figure 3b is the $2p_\pi$ ($4b_2$) orbital on NH_2. Table 2 shows that this is indeed the case in the $^2B_2$ ground state of the complex. Occupying this strongly antibonding orbital by two electrons gives rise to rather large excitation energies for the resulting states: $^2A_1$, $^2B_1$, and $^2B_2$. Of these states the lowest is $^2A_1$ because it involves a hole in the second highest orbital of the 3d orbitals, namely d_{z^2} ($10a_1$). All the entries for $[CuNH_2]^+$ in Table 2 confirm the orbital schema as presented in Figure 3b and derived in the previous paragraph on the basis of the results for $[NiNH_2]^+$. Our CASPT2 value of 51.64 kcal/mol is about 6 kcal/mol larger than the experimental value of 45.9 kcal/mol. The B3LYP value of 41.7 kcal/mol is smaller by roughly the same amount.[10] We conclude therefore that the experimental recommended binding energy is to a large extent confirmed by the present calculations.

Conclusions

Detailed analysis of the low-lying states of the amide complexes $[MNH_2]^+$ have clearly demonstrated a different bonding pattern for the early and middle first-row transition cations (Sc^+-Co^+) on one hand and the late transition metal complexes (Ni^+ and Cu^+) on the other hand. The ground states of the former complexes correspond to a formal transfer of a metal electron to the $2p_\pi$ orbital of NH_2. Opposed to this transfer, donation of charge from the ligand to the metal takes place in the low-lying predominantly sp^2 and $2p_\pi$ ligand orbitals, resulting in a total charge on the metal cation that is only somewhat larger than 1. The ligand $2p_\pi$ orbital exhibits a strong bonding character with respect to the metal ligand bond, which places the 3d level of the metal cation well above the ligand orbitals. The antibonding effects in the 3d orbitals are by far more pronounced in the π-type orbital (d_{yz}) than in the σ-type orbital (d_{z^2}). This makes the $M-NH_2$ bonding rather exceptional in transition metal chemistry and as matter of fact in chemistry as a whole. An explanation of this extraordinary result lies in a relatively low-lying σ valence ligand orbital (sp^2 lone pair orbital on N) as compared to the $2p_\pi$ (NH_2) and 3d (M^+) orbitals. The low-lying states of the $[MNH_2]^+$ complexes of Cu^+ and Ni^+ have a quite different electronic structures. The origin of this difference lies in the stabilization of the 3d orbitals when going from left to the right along the first-row transition metal cations M^+. As a consequence, the 3d orbitals of Cu^+ and Ni^+ are situated below the $2p_\pi$ orbital of NH_2, causing this orbital to become a singly occupied antibonding HOMO in the ground states of the corresponding amide complexes. Although in the d orbitals the π interactions are still stronger than σ interactions, the importance of the latter effect increases steadily along (left to right) the first-row transition metal $[MNH_2]^+$ complexes. All complexes studied have in common that there exists π bonding between the metal and the ligand, which forces their structures to be planar. Indeed, B3LYP geometry optimizations give without any exception planar structures. After correcting for zero-point vibrational energies and including relativistic effects, CASPT2 binding energies compare in most cases reasonably well with the experimental values. Unexpected deviations are calculated for the V^+, Co^+, and Ni^+ amide complexes, for which further experimental and theoretical work is needed to solve the discrepancies. However, the qualitative trend that is experimentally observed across the first-row transition metal series is reproduced entirely by our CASPT2 calculations.

Acknowledgment. Financial support by the Flemish Science Foundation and the Flemish Government under the Concerted Action Scheme is gratefully acknowledged.

References and Notes

(1) Clemmer, D. E.; Armentrout, P. B. *J. Phys. Chem.* **1991**, *95*, 3084.
(2) Clemmer, D. E.; Sunderlin, L. S.; Armentrout, P. B. *J. Phys. Chem.* **1990**, *94*, 3008.
(3) Clemmer, D. E.; Sunderlin, L. S.; Armentrout, P. B. *J. Phys. Chem.* **1990**, *94*, 208.
(4) Liyanage, R.; Armentrout, P. B. *Int. J. Mass Spectrom.* **2005**, *241*, 243.
(5) Mavridis, A.; Herrera, F. L.; Harrison, J. F. *J. Phys. Chem.* **1991**, *95*, 6854.
(6) Kapellos, S.; Mavridis, A.; Harrison, J. F. *J. Phys. Chem.* **1991**, *95*, 6860.
(7) Taketsugu, T.; Gordon, M. S. *J. Chem. Phys.* **1997**, *106*, 8504.
(8) Hendrickx, M.; Ceulemans, M.; Gong, K.; Vanquickenborne, L. *J. Phys. Chem. A* **1997**, *101*, 8540.
(9) Nakao, Y.; Taketsugu, T.; Hirao, K. *J. Chem. Phys.* **1999**, *110*, 10863.
(10) Michelini, M. D. C.; Russo, N.; Sicilia, E. *Inorg. Chem.* **2004**, *43*, 4944.
(11) Michelini, M. D.; Sicilia, E.; Russo, N.; Alikhani, M. E.; Silvi, B. *J. Phys. Chem. A* **2003**, *107*, 4862.
(12) Michelini, M. D.; Russo, N.; Sicilia, E. *J. Phys. Chem. A* **2002**, *106*, 8937.
(13) Sicilia, E.; Russo, N. *J. Am. Chem. Soc.* **2002**, *124*, 1471.
(14) Russo, N.; Sicilia, E. *J. Am. Chem. Soc.* **2001**, *123*, 2588.
(15) Chiodo, S.; Kondakova, O.; Michelini, M. D.; Russo, N.; Sicilia, E.; Irigoras, A.; Ugalde, J. M. *J. Phys. Chem. A* **2004**, *108*, 1069.
(16) Frisch, M. J.; Trucks, G. W.; Schlegel, H. B.; Scuseria, G. E.; Robb, M. A.; Cheeseman, J. R.; Montgomery, J. A.; Vreven, J., T.; Kudin, K. N.; Burant, J. C.; Millam, J. M.; Iyengar, S. S.; Tomasi, J.; Barone, V.; Mennucci, B.; Cossi, M.; Scalmani, G.; Rega, N.; Petersson, G. A.; Nakatsuji, H.; Hada, M.; Ehara, M.; Toyota, K.; Fukuda, R.; Hasegawa, J.; Ishida, M.; Nakajima, T.; Honda, Y.; Kitao, O.; Nakai, H.; Klene, M.; Li, X.; Knox, J. E.; Hratchian, H. P.; Cross, J. B.; Adamo, C.; Jaramillo, J.; Gomperts, R.; Stratmann, R. E.; Yazyev, O.; Austin, A. J.; Cammi, R.; Pomelli, C.; Ochterski, J. W.; Ayala, P. Y.; Morokuma, K.; Voth, G. A.; Salvador, P.; Dannenberg, J. J.; Zakrzewski, V. G.; Dapprich, S.; Daniels, A. D.; Strain, M. C.; Farkas, O.; Malick, D. K.; Rabuck, A. D.; Raghavachari, K.; Foresman, J. B.; Ortiz, J. V.; Cui, Q.; Baboul, A. G.; Clifford, S.; Cioslowski, J.; Stefanov, B. B.; Liu, G.; Liashenko, A.; Piskorz, P.; Komaromi, I.; Martin, R. L.; Fox, D. J.; Keith, T.; Al-Laham, M. A.; Peng, C. Y.; Nanayakkara, A.; Challacombe, M.; Gill, P. M. W.; Johnson, B.; Chen, W.; Wong, M. W.; Gonzalez, C.; Pople, J. A. *Gaussian 03*; Gaussian Inc.: Pittsburgh, 2003.
(17) Karlström, G.; Lindh, R.; Malmqvist, P.-Å.; Roos, B. O.; Ryde, U.; Veryazov, V.; Widmark, P.-O.; Cossi, M.; Schimmelpfennig, B.; Neogrady, P.; Seijo, L. MOLCAS 6.2. *Comput. Mater. Sci.* **2003**, *28*, 222.
(18) Roos, B. O.; Lindh, R.; Malmqvist, P. A.; Veryazov, V.; Widmark, P. O. *J. Phys. Chem. A* **2005**, *109*, 6575.
(19) *Organometallic Ion Chemistry*; Armentrout, P. B., Kickel, B. L., Freiser, B. S., Eds.; Kluwer Academic Publishers: Dordrecht, 1996.
(20) Johns, J. W.; Ramsey, D. A.; Ross, S. C. *Can. J. Phys.* **1976**, *54*, 1804.